

# SILICON SUBSTRATE INTEGRATED HIGH Q-FACTOR PARALLEL-PLATE FERROELECTRIC VARACTORS FOR MICROWAVE/MILLIMETERWAVE APPLICATIONS

A. Vorobiev<sup>1</sup>, P. Rundqvist<sup>1</sup>, K. Khamchane<sup>1</sup>, and S. Gevorgian<sup>1,2</sup>

andrei.vorobyev@ep.chalmers.se

parru@ep.chalmers.se

khaled@fy.chalmers.se

spartak@ep.chalmers.se

<sup>1</sup>Chalmers University of Technology, SE-41296 Göteborg, Sweden

<sup>2</sup>Microwave and High Speed Electronics Research Center, Ericsson AB, 431 84 Mölndal, Sweden

## ABSTRACT

Parallel-plate  $\text{Ba}_{0.25}\text{Sr}_{0.75}\text{TiO}_3$  (BST) varactors with record high Q-factor are fabricated on Si substrate. At 45 GHz the Q-factor is about 40 and tuneability at 25 V is more than 40 % in the measured frequency range 0.045-45 GHz. These parameters are comparable or far better than corresponding parameters of best Si and GaAs analogues. The improvement in Q-factor is achieved by using thick bottom electrode consisting of Pt(50 nm)/Au(0.5  $\mu\text{m}$ ) allowing to reduce the microwave losses in metal layers. However, the measured loss tangent of varactor is about one order of magnitude more than  $\text{SrTiO}_3$  single crystal, indicating that there is a room for further improvement of the Q-factor. The analysis of dielectric dispersion of BST film allows to assume that the dielectric loss is associated with charged defects. The dc current through varactor is found to be controlled by Poole-Frenkel mechanism associated with the field enhanced thermal excitation of charge carriers from internal traps, possibly ascribed to be oxygen vacancies. The varactors can be used above 10 GHz to develop different high performance tuneable microwave devices integrated with Si substrates.

Thin  $\text{Ba}_x\text{Sr}_{1-x}\text{TiO}_3$  (BST) films have been extensively considered for applications in voltage controlled microwave devices (e.g. varactors).<sup>1,2</sup> However, relatively high losses have limited large-scale industrial applications of these devices. Additionally, from industrial perspective, it is important to integrate these devices with Si substrate and reduce required control voltages. In comparison with co-planar design<sup>1,3</sup> the devices with parallel-plate electrodes<sup>2,4</sup> offer lower control voltage and higher tuneability. The Q-factor of BST varactors on Pt/Si substrates is limited mainly by the losses in bottom Pt electrodes<sup>5,6</sup> which is usually 100-200 nm thick.<sup>2,7</sup> To reduce these losses bottom electrodes made of thick Pt (up to 2  $\mu\text{m}$ )<sup>5</sup>, Au<sup>8</sup>, and Cu<sup>9</sup> have been proposed. However, no Q-factor or/and tuneability of these varactors at microwave frequencies are reported explicitly. In this paper, we present the results of fabrication and microwave characterization of record high Q-factor parallel-plate BST varactors on Si substrate with thick Pt/Au bottom electrode. The Q-factor and the tuneability of these varactors are comparable or far better than the corresponding parameters of best GaAs and Si analogues. The simultaneous analysis of the microwave dielectric response and dc conduction mechanism of Au/BST/Au varactor allows to suggest the predominant mechanism of the extrinsic microwave loss and corresponding BST film microstructure imperfections.

Oxidized n-type silicon (100)Si ( $\rho = 5 \text{ k}\Omega\cdot\text{cm}$ ) with adhesive  $\text{TiO}_2$  (15 nm) and Pt (100 nm) layers are used as substrate. To complete the bottom electrode a 0.5  $\mu\text{m}$  thick Au film, and a 50 nm Pt layer are deposited by e-beam evaporation at room temperature. This structure forms BST/Pt/Au varactors. For comparison, Pt(200 nm)/ $\text{TiO}_2/\text{SiO}_2/\text{Si}$  structures are used as substrate to form BST/Pt varactors. BST films (300 nm thick) are grown by laser ablation of  $\text{Ba}_{0.25}\text{Sr}_{0.75}\text{TiO}_3$  target. To keep the parallel-plate structure symmetric a 50 nm Pt and a 0.5  $\mu\text{m}$  Au layers are deposited on BST film by e-beam evaporation. Top electrodes are patterned by lift-off process.

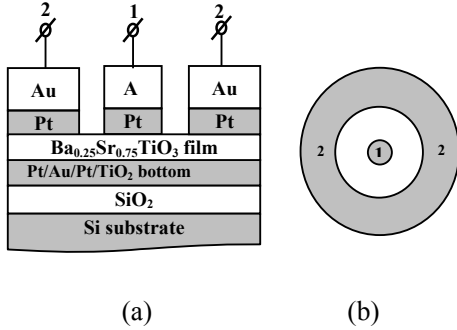


Fig. 1. Cross section (a) and layout of top electrodes (b) of BST varactor.

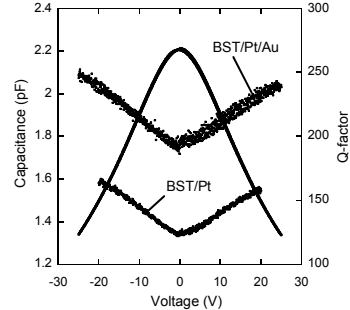


Fig. 2. Capacitance- and Q-factor-voltage dependencies of BST/Pt/Au varactor at 1.0 MHz. Shown are also Q-factor of a BST/Pt varactor with thin (only 200 nm Pt) bottom electrode.

The cross section of the varactor and layout of the top electrodes are shown in Fig. 1. Due to the large area (compared with central circular top electrode) and hence large capacitance the external top electrode 2 provides effective DC and microwave “connection” to the bottom plate.

Fig. 2 shows the typical C-V and Q-factor of a 30 μm BST/Pt/Au varactor at 1.0 MHz. The C-V has no butterfly shape indicating that the BST films are in the paraelectric phase. It can be seen that the capacitance is not saturated even at 25 V (830 kV/cm), and further decrease of the capacitance may be expected. For comparison, the Q-factor of a BST/Pt (only 200 nm Pt as bottom electrode) varactor is shown.

Fig. 3 shows the frequency dependences of capacitance of BST/Pt/Au varactor and permittivity of BST film, extracted from measured impedance.<sup>10</sup> The permittivity is about 150 and it is fairly frequency independent up to 45 GHz (maximum measured frequency). The observed frequency dispersion of capacitance is explained by influence of parasitics (inductance, capacitance) of device electrodes (Fig. 1). Under 25 V the tuneability of capacitance and permittivity is more than 40% in the whole frequency range.

Fig. 4 shows the Q-factor frequency dependences of the 10 μm BST/Pt and BST/Pt/Au varactors. The glitches at 10 GHz are due to the uncertainty of calibrations. At 10 GHz the Q-factor of BST/Pt/Au varactor is about 100. For comparison, Fig. 4 shows the Q-factors of the best reported semiconductor varactors calculated using  $1/\omega$  low. At 45 GHz the Q-factor of BST/Pt/Au varactor is comparable with GaAs dual Schottky diode (cut-off frequency of 2.4 THz). It can be seen from Fig. 4 that at 45 GHz the Q-factor of GaAs heterostructure-barrier-varactor (HBV) is almost 5 times smaller than Q-factor of our BST/Pt/Au varactor. The Q-factor of Si abrupt junction varactor diode is even smaller. The high Q-factor of BST/Pt/Au varactor, in comparison with BST/Pt, may be explained by reduced microwave losses in thicker bottom electrode, which in addition has higher conductivity.

The  $\tan\delta(1/Q)$  of BST/Pt/Au varactor is substantially low, however, one order of magnitude more than SrTiO<sub>3</sub> single crystal.<sup>11</sup> It is worthwhile to identify the predominant loss mechanism and corresponding film defects with the aim to improve the film microstructure and reduce the dielectric losses. The known extrinsic loss mechanisms, considered as essentially contributing, are systemized by Tagantsev<sup>12</sup> and Vendik<sup>13</sup> : (i) loss owing to charged defects, (ii) universal relaxation law mechanism, (iii) quasi-Debye contribution induced by random -field defects. Above 10 GHz loss tangent is approximately linear with frequency and changes versus dc bias nearly proportionally to the permittivity of material (Fig. 3). These features can be attributed only to the charged defects loss mechanism<sup>12</sup> above the relaxation frequency (about 10 GHz<sup>13</sup>).

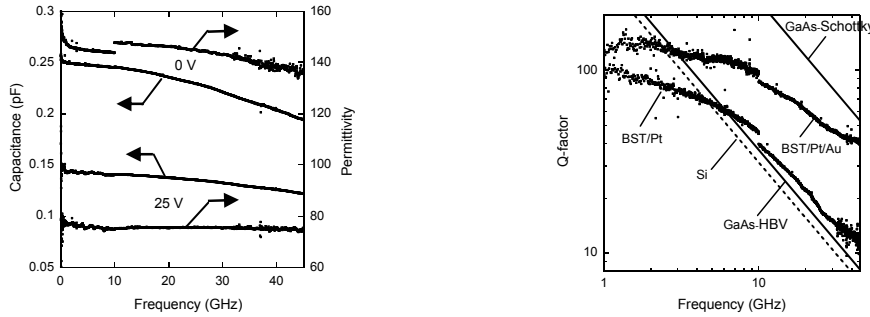


Fig. 3. Frequency dependencies of capacitance and permittivity of BST/Pt/Au varactor at  $V=0$ , and 25 V.

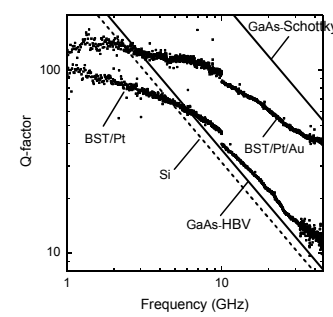


Fig. 4. Frequency dependencies of Q-factor of BST/Pt/Au and BST/Pt varactors at zero bias. Shown are also Q-factors of: Si abrupt junction varactor (Metelics, MSV34,060-C12,  $Q=6500$  @ 50 MHz,  $V=-4V$ ), GaAs HBV (Darmstadt University of Technology),  $f_{\text{cut-off}}=370$  GHz, and GaAs dual Schottky diode (United Monolithic Simiconductors, DBES105a,  $f_{\text{cut-off}}=2.4$  THz).

An another way to detect defects is to analyze dc current through the ferroelectric film, which in the nonlinear regime is normally ascribed to either the Pool-Frenkel (PF) or Schottky emission conduction mechanisms.<sup>14,15</sup> The I-V dependencies of our BST varactors reveal the nonlinear regime at fields up to 200 kV/cm followed by the low ohmic region at fields up to 800 kV/cm. Fig. 5 shows the nonlinear current regime with  $J/E$  vs  $E^{1/2}$ . The measured slope is found to be about  $1.66 \cdot 10^{-3} \text{ C.J}^{-1} \cdot \text{V}^{1/2}$  which is very close to the value calculated using PF low ( $1.57 \cdot 10^{-3} \text{ C.J}^{-1} \cdot \text{V}^{1/2}$ ).<sup>16</sup> This fact indicates that at fields below 200 kV/cm the current is controlled by PF (trapping/detrapping) conduction mechanism usually attributed to the current induced by grain boundary defects, mainly by positively charged oxygen vacancies acting as internal traps.<sup>17</sup> The following low ohmic region can be explained by field assisted lowering of the trap barriers.<sup>18</sup> The resistivity estimated from the Ohmic I-V region is  $\rho \approx 10^{10} \Omega \text{ cm}$ , as in a good quality single crystal  $\rho \geq 10^9 \Omega \text{ cm}$ .<sup>19</sup> Thus, the analysis of dc current through BST varactor confirms the presence of charged defects which are usually considered to be oxygen vacancies formed at grain boundaries.<sup>17</sup>

In conclusion, we have demonstrated record high Q-factor parallel-plate BST varactors fabricated on thick bottom Au/Pt electrode integrated with Si substrate. In the frequency range 5–40 GHz the Q-factor of BST varactors is more then 50 which is comparable or larger then Q-factors of the best semiconductor analogues. The tuneability of BST varactors at 25 V is more than 40 % in the whole frequency range 1 MHz-45 GHz. With these parameters the BST varactors may compete semiconductor varactors in tunable microwave devices above 10-20 GHz. Additionally, ferroelectric varactor has symmetric C-V characteristic, as HBV, and extremely small leakage current. For example, the current through our 10  $\mu\text{m}$  BST/Pt/Au varactor at 20 V is about  $5 \cdot 10^{-11} \text{ A}$  that is 3 order of magnitude less than reverse current through dual Schottky diode at 5V.

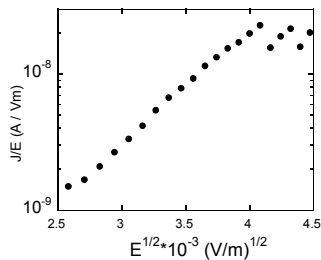


Fig. 5. The nonlinear regime of current through BST/Pt/Au varactor plotted as current density-field ratio  $J/E$  versus square root of field  $E^{1/2}$ .

The loss tangent is about an order of magnitude larger than in single crystals (e.g. SrTiO<sub>3</sub>), indicating that there is a room for further improvement of the films/varactors. The analysis of frequency and field dielectric dispersion shows that the extrinsic microwave loss in FE film can be attributed to the charged defects. The dc current through varactor is found to be controlled by Poole-Frenkel mechanism associated with hopping charge carriers by internal traps which usually are the positively charged oxygen vacancies at grain boundaries. This confirms the conclusion about extrinsic microwave loss due to charged defects mechanism. The plans for the nearest future include the optimization of BST varactor structure formation with the aim to minimize the amount of charged defects and further improve the varactor performance.

This work was supported by the Swedish Strategic Research Foundation SSF (OXIDE and HFE programs), and Chalmers Center for High Speed Technology.

## REFERENCES

- <sup>1</sup> W. J. Kim, W. Chang, S. B. Qadri, J. M. Pond, S. W. Kirchoefer, D. B. Chrisey, and J. S. Orwitz, *Appl. Phys. Lett.* **76**, 1185 (2000).
- <sup>2</sup> R.A. York, A.S. Nagra, P. Periaswamy, O. Auciello, S.K. Streiffer and J. Im, *Journal of Integrated Ferroelectrics* **34**, 177 (2000).
- <sup>3</sup> S. Abadei, S. Gevorgian, C.-R. Cho, and A. Grishin, *J. Appl. Phys.* **91**, 2267 (2002).
- <sup>4</sup> A. Tombak, J.-P. Maria, F. Ayguavives, Z. Jin, G. T. Stauf, A. I. Kingon, and A. Mortazawi, *IEEE Microwave and Wireless Comp. Lett.* **12**, 3 (2002).
- <sup>5</sup> G. T. Stauf, C. Ragaglia, J. F. Roeder, D. Vestyeck, J.-P. Maria, T. Ayguavives, A. Kingon, A. Mortazawi, and A. Tombak, *Integr. Ferroel.* **39**, 321 (2001).
- <sup>6</sup> D. C. Dube, J. Baborowski, P. Muralt, and N. Setter, *Appl. Phys. Lett.* **74**, 3546 (1999).
- <sup>7</sup> B. A. Baumert, L.-H. Chang, A. T. Matsuda, T.-L. Tsai, C. J. Tracy, R. B. Gregory, P. L. Fejes, N. G. Cave, W. Chen, D. J. Taylor, T. Otsuki, E. Fujii, S. Hayashi, and K. Suu, *J. Appl. Phys.* **82**, 2558 (1997).
- <sup>8</sup> B. Acikel, T. R. Taylor, P. J. Hansen, J. S. Speck, and R. A. York, *IEEE Microwave and Wireless Comp. Lett.* **12**, 237 (2002).
- <sup>9</sup> W. Fan, S. Saha, J. A. Carlisle, O. Auciello, R. P. H. Chang, and R. Ramesh, *Appl. Phys. Lett.* **82**, 1452 (2003).
- <sup>10</sup> P. Rundqvist, A. Vorobiev, S. Gevorgian, and K. Khamchane, submitted to *Integr. Ferroel.*
- <sup>11</sup> G. Rupprecht and R. O. Bell, *Phys. Rev.* **125**, 1915 (1962).
- <sup>12</sup> A. K. Tagantsev, V. O. Sherman, K. F. Astafiev, J. Venkatesh and N. Setter, to be published in *Journal of Electroceramics*.
- <sup>13</sup> O. G. Vendik, S. P. Zubko, and M. A. Nikol'ski, *J. Appl. Phys.* **92**, 7448 (2002).
- <sup>14</sup> P. Li and T.-M. Lu, *Phys. Rev. B*, **43**, 14 261 (1991).
- <sup>15</sup> Sufi Zafar, Robert E. Jones, Bo Jiang, Bruce White, V. Kaushik, and S. Gillespie, *Appl. Phys. Lett.* **73**, 3533 (1998).
- <sup>16</sup> S. M. Sze, *Physics of Semiconductor Devices*, 2<sup>nd</sup> ed. (Wiley, New York, 1981).
- <sup>17</sup> Yin-Pin Wang and Tseung-Yuen Tseng, *J. Appl. Phys.* **81**, 6762 (1997).
- <sup>18</sup> M. S. Tsai and T. Y. Tseng, *Mat. Chem. Phys.* **57**, 47 (1998).
- <sup>19</sup> Landolt-Börnstein, *Numerical Data and Functional Relationship in Science and Technology*, Springer-Verlag Berlin, 1981.